NANO LETTERS

pubs.acs.org/NanoLett

Finite Curvature-Mediated Ferroelectricity

Stephen S. Nonnenmann, Oren D. Leaffer, Eric M. Gallo, Michael T. Coster, and Jonathan E. Spanier*

Department of Materials Science and Engineering, Department of Electrical and Computer Engineering, and Drexel University, Philadelphia, Pennsylvania 19104

ABSTRACT We demonstrate that ferroelectric (FE) polarizations oriented along the finite thickness direction in ultrathin films are enhanced by the introduction of extreme curvature, thereby suppressing the finite-size-driven evolution of the FE phase transition temperature T_C. The measured responses within individual nanoshells possess magnitudes nearly three times that for their planar counterparts while exhibiting finite curvature-dependent offsets in FE switching hystereses. In stark contrast to the expected scaling of a depression of T_C with inverse thickness, results based on modified Landau−Ginzburg model calculations indicate geometric curvature-driven polarization gradients in ultrathin films result in significant increases in T_C.

KEYWORDS Ferroelectric nanotube, core−shell nanowire, finite curvature, piezoresponse

Ferroelectric (FE) thin films and nanostructures continue to attract intense interest[1−5] for their enormous potential as highly versatile nonvolatile memory elements,[1,6−8] for terahertz emission and thermocaloric cooling,[9] and for their finite size-dependent physical phenomena.[2,3,5,8,10,11] The stability of the FE phase in ultrathin films and nanostructures is limited by the relative contribution of the depolarizing field to the free energy, arising from incomplete screening of surface polarization charge. Extreme reduction in film thicknesses is typically accompanied by a concomitant decrease in FE polarization P and phase transition temperature T_C, reflecting a critical size for ferroelectricity. In recent years efforts to develop strategies to stabilize switchable FE states in few-monolayer films via heteroepitaxial strain,[1,4,6] surface chemical environment,[5] and selection of FE−metal interfaces[12] hold great promise for addressing finite-size limitations, further demonstrating the significance of the surface and interfacial boundary conditions.

The deleterious effect of the depolarizing field is equally severe for FE nanoparticles, but FE nanoparticles can exhibit unexpected and new physical phenomena not found in bulk. For example, toroidal FE ordering[10,13] and enhancements in axially oriented polarization P_z and in T_C in FE nanotubes and nanowires owing to electrostrictive coupling of azimuthal stresses[11,14] have been reported, suggesting new possibilities for high-density encoding of information. Experimental evidence indicates that polarizations oriented either parallel[15] or perpendicular[8,16] to the FE oxide nanowire axes are stable and switchable.

In this Letter we present evidence for suppression of the finite-size reduction of FE polarizations in ultrathin and extremely curved nanoshells with polarizations oriented along shell inward and outward normals. Significantly we demonstrate that such curvature can alter the evolution of T_C, providing a new means of circumventing finite-size limitations. Local FE switching and piezoelectric responses within individual, coaxial cylindrical oxide perovskite ($PbZr_{0.52}Ti_{0.48}O_3$,PZT) nanoshells each encasing a noble-metal (Au) core[17] were probed using piezoelectric force microscopy (PFM)[18] collected in the atmosphere at room temperature (Figure 1a). Measurements collected from a range of thicknesses and radii indicate remarkably large responses compared to their planar counterparts of identical composition. Significantly, no systematic decrease in the FE response is seen for decreasing shell thickness.

Shown in parts b−e of Figure 1 are traces of the real part of the radial component of the displacement, i.e., local FE piezoelectric hysteresis loops for PZT nanoshells possessing selected values of inner radius a and shell thickness ζ. A representative trace of the variation of the cantilever phase during collection of ferroelectric piezoelectric hysteresis loops of an $a = 18$ nm, $\zeta = 7$ nm nanoshell is shown in the upper left inset of Figure 1a. Figure 2a summarizes the d_{33} responses in each nanoshell, comparing to measured responses in planar thin films (dotted gray) and calculated radially oriented polarizations (dotted blue). Locally measured effective d_{33} values in the switching in thin film and nanostructured FEs are related to the local FE polarization through the product of the electrostriction coefficient and dielectric susceptibility,[18,19] i.e., $d_{33} \approx 2Q_{11}\chi_{33}P$. Calibrated d_{33} values were referenced to measured cantilever stiffnesses obtained from force−distance responses. Significantly, the remanent polarizations observed here do not exhibit a systematic decrease for decreasing values of ζ or outer radius b, in stark contrast to previous reports of a linear reduction for logarithmically decreasing values of film thicknesses.[20] Although our estimate of d_{33} can be expected to be influenced by the nonuniform local electric field in the proximity of the cantilever tip, the measured response for

* To whom correspondence should be addressed, spanier@drexel.edu.
Received for review: 10/10/2009
Published on Web: 01/12/2010

DOI: 10.1021/nl903384p | *Nano Lett.* **2010,** *10,* 542-546

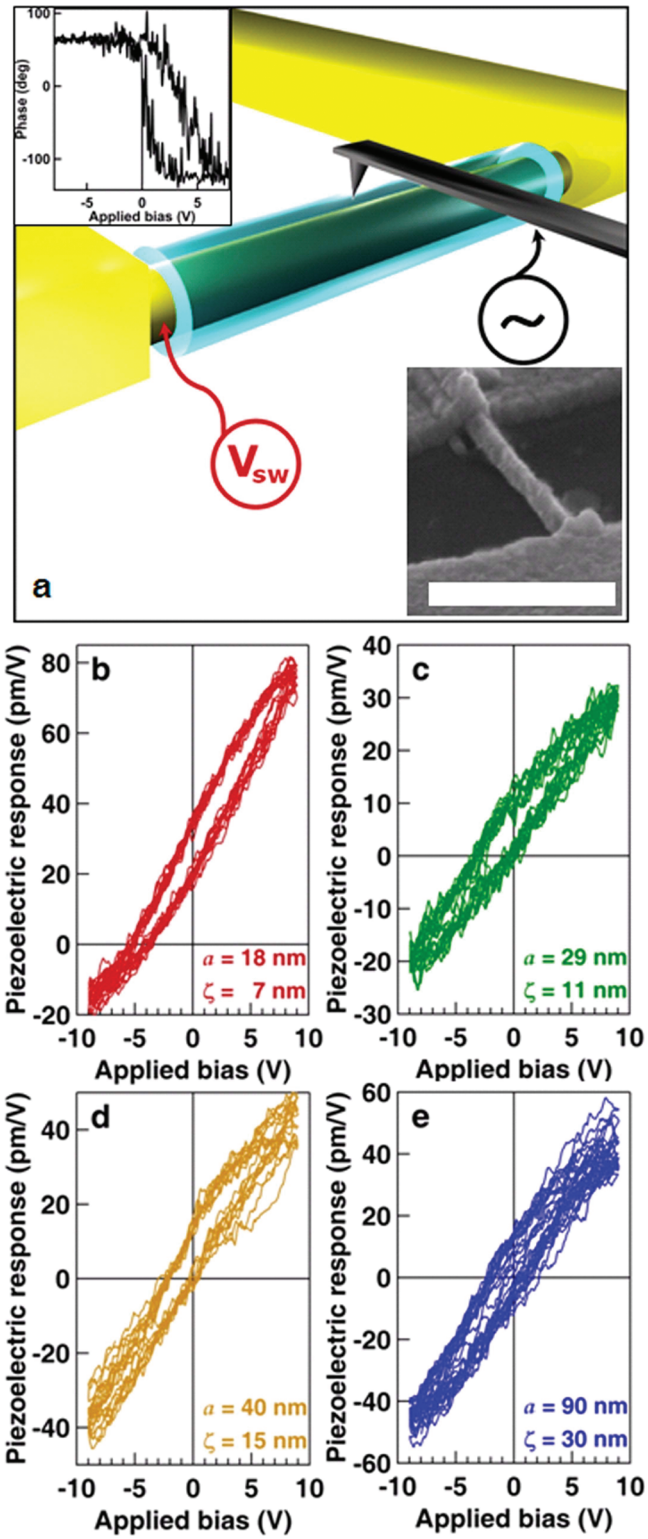

FIGURE 1. (a) Illustration of the electrically interfaced nanoshell and measurement, along with an the electron micrograph of a representative nanowire (inset scale bar ~1 μm). (b–e) Measured FE piezoelectric hysteresis loops collected from the oxide perovskite nanoshells, for shell thicknesses ζ and corresponding inner radii a as denoted in the legend. The inset in the upper left of (a) is a plot of the measured phase response of a shell as a function of voltage bias applied across its wall, indicating ferroelectric switching of the shell polarization.

the $\zeta = 7$ nm, $a = 18$ nm shell is nevertheless ~300% that of an epitaxially grown planar thin film of identical composition that is ~60% thicker (Figure 2a) as measured and reported using the same method.[20] (See Supporting Information for details of the measurement configuration and analysis).

The present results are noteworthy in light of the expected linear decrease in piezoelectric response in planar thin films with increasing electric field intensity.[21] On the basis of estimates of FE domain sizes induced and switched in films by a proximal probe, and noting the geometric confinement of the domain provided by the shell diameter and thickness, we estimate that the smallest for which we observe switchable FE domains in these nanoshells to be ~6000 nm^3. An extrapolation of these experimental results to thinner shells possessing comparable values of ζ/b suggests that switchable and stable radial FE polarizations may be retained in thinner shells and, significantly, those situated within real metal electrodes with finite screening lengths. Reduction in film thickness is typically accompanied by an increase in the coercive field E_C; this effect in films as thin as ~100 nm has been attributed to charge injection through a non-FE layer at the film/electrode interface.[22] Absent a priori knowledge of the extent of coverage and the character of molecular adsorbates between the probe tip and the shell surface, we estimate $E_C \approx 3800$ kV/cm for $\zeta = 7$ nm and $b = 25$ nm. While this value is much larger than that for a planar film of identical composition and comparable thickness ($E_{C,film} \approx 1200$ kV/cm for 8 nm thick film) and the value of the intrinsic thermodynamic limit ($E_{C,thermo} \approx 1200$ kV/cm),[21] both the experimental data and the results of our model calculations exhibit a $E_C \sim \zeta^{-1}$ scaling (Figure 2b). The data also show curvature- and shell-thickness-dependence of the horizontal and vertical offsets of the hysteresis loops. Plotted in parts c and d of Figure 2 are the center-of-switching (COS) offsets along the piezoresponse and voltage axes, respectively, for selected values of b.

What is the origin of the unexpectedly large FE response in these ultrathin nanoshells along their smallest dimension, and of the offsets of the FE hysteresis loops? Our theoretical analyses of their radially oriented polarization profiles P_r indicate thermodynamic stability with finite diameter- and shell-thickness-dependent enhancements in P_r and T_C. In thin film FE capacitors, an in-plane compressive strain near one or both interfaces, or a strain gradient normal to the plane of the film (e.g., from composition, thermal stresses or bending curvature) couple to P, altering its magnitude, T_C, dielectric tunability, and pyroelectric response.[23] Our model description (Figure 3b, inset) is that of a coaxial cylindrical FE capacitor that is comprised of a noble metal (Au core surrounded by a FE oxide perovskite (PZT) shell of inner and outer radii a and b, respectively, where ρ is defined as the radial position

DOI: 10.1021/nl903384p | *Nano Lett.* **2010,** *10,* 542-546

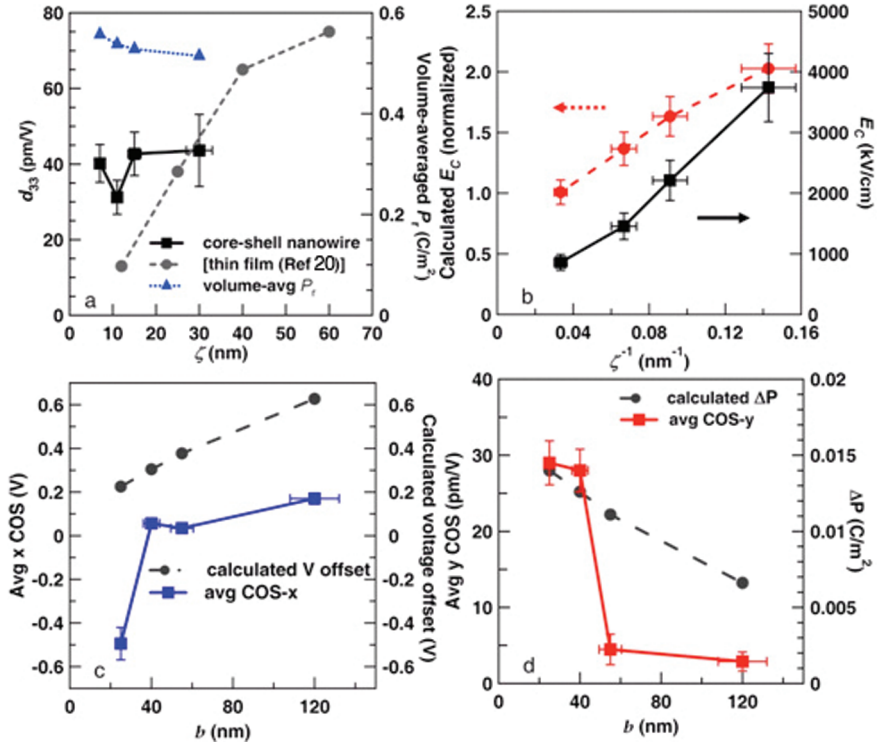

FIGURE 2. (a) Measured variation of the FE piezoelectric response with curvature, compared with those for planar thin films of identical composition (ref 20), and a scatter plot of the calculated volume-averaged polarization (right axis). (b) Coercive electric field E_C plotted as a function of shell thickness $\zeta = b - a$. (c) Measured vertical center-of-switching (COS) offset values of the FE hysteresis for each nanoshell. (d) Horizontal (voltage) COS offsets (solid squares connected by solid lines), plotted as a function of nanoshell outer radius b. Also shown in (c) and (d), respectively, are the corresponding calculated polarization and voltage offsets.

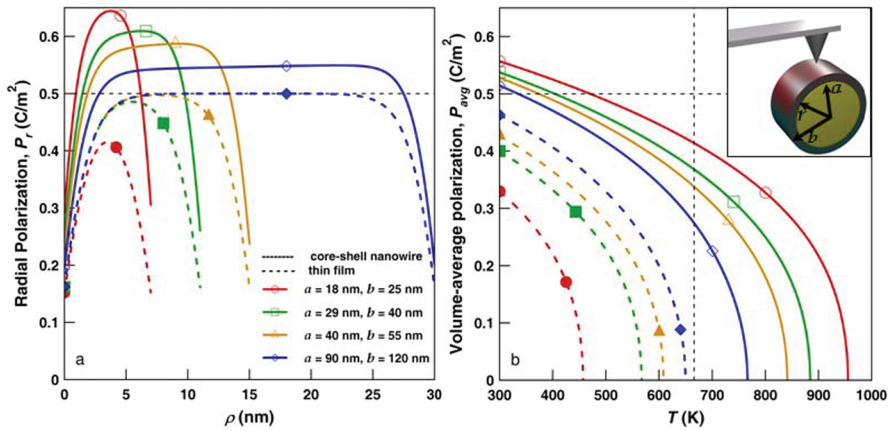

FIGURE 3. (a) Calculated (300 K) radial polarization profile ρ for selected values of shell inner and outer radii a and b, respectively (solid lines), and for planar, stress-free thin films of corresponding thicknesses (dashed lines). (b) Calculated volume-averaged P_r as a function of temperature for the nanoshells of selected diameters and thicknesses (solid lines), and for planar, stress-free thin films of corresponding thicknesses (dashed lines) plotted in (a); the inset illustrates the model geometry. In (a) and (b) the bulk polarization value is denoted by horizontal dashed black lines, and in (b) the bulk T_C value is denoted by a vertical dashed line.

within the shell. With surface tension of $\mu = 5$ N/m,[11] the calculation of the radial dependence of the radial and azimuthal stresses (σ_{rr} and $\sigma_{\varphi\varphi}$, respectively) and within the shell subject to these surface tensions is of the form of a Lamé problem. Specifically, application of surface boundary conditions $\sigma_{rr}(b) = p_{b\rho}$ $(= \mu/b)$, $-\sigma_{rr}(a) = p_{a\rho}$ $(= \mu/a)$, and of mechanical equilibrium $\partial\sigma_{ij}/\partial x_j = 0$ lead to

$$\sigma_{rr,\varphi\varphi}(r) = \frac{a^2}{b^2 - a^2}\left(1 \mp \frac{b^2}{r^2}\right)p_{a\rho} - \frac{b^2}{b^2 - a^2}\left(1 \mp \frac{a^2}{r^2}\right)p_{b\rho} \quad (1)$$

To calculate the radial polarization $P_r(r,a,b)$ and evolution of $T_C(a,b)$ we modify the Landau−Ginzburg formalism, writing the

volumetric and surface portions of the Gibbs free energy per unit length, assuming axisymmetric radial polarization $P_r(r)$

$$G = \int_a^b \left[\frac{\hat{A}}{2}P_r(r)^2 + \frac{B}{4}P_r(r)^4 + \frac{C}{6}P_r(r)^6 + \frac{1}{2}g(\nabla P_r)^2 - E_d(r)P_r(r)\right] r\,dr + \int_S P_r^2\,dS \quad (2)$$

where $\hat{A}(r) = A - 2Q_{11}\sigma_{rr}(r) - 2Q_{12}\sigma_{\varphi\varphi}(r)$ is the renormalized Landau stiffness, $A = A_0(T - T_C)$, A_0, B,, and C are defined for $PbZr_{0.52}\,Ti_{0.48}\,O_3$,[24] g (=1 nm) is the energetic cost associated with variation of P_r near the surface,[11] and $E_d(r)\,P_r(r)$ is the depolarizing field contribution. Q_{11} and Q_{12} are the electrostrictive coefficients for this composition of PZT.[24,25] We approximate the depolarizing field, self-consistently, using the form[26] $E_d(r) = 4\pi[P_r(r) - \bar{P}_r]$, i.e., where $\bar{P}_r$ represents the averaged polarization across the nanoshell thickness. Sets of $P_r(\rho)$ were obtained by numerical integration of the resulting Euler–Lagrange equation $g\nabla^2 P_r(r) = \hat{A}P_r(r) + BP_r^3(r) + CP_r^5(r) - E_d(r)$ via a nonlinear finite-difference method, subject to the electrostatic boundary conditions $(dP_r/dr - g^{-1}P_r)|_{r=a} = (dP_r/dr + g^{-1}P_r)|_{r=b} = 0$. (See Supporting Information for additional details pertaining to the model calculations.)

Plots of calculated $P_r(\rho)$ at 300 K for selected pairs of values of a and b are shown in Figure 3a along with the calculated P_r versus position for planar, stress-free films of corresponding thicknesses. The polarization profiles for the shells possess distinct curvature- and shell-thickness-dependent asymmetric variation, with higher peak polarizations than their planar counterparts. Plotted in Figure 3b is a series of calculated results showing the variation of volume-averaged P_r with temperature for these radius and thickness combinations, including those for planar stress-free films of corresponding thicknesses. Remarkably, the expected finite thickness-dependent reduction in P_r and evolution in T_C are completely suppressed; compared with the planar films of identical thickness, a calculated ~500 K increase for the highest-curvature and thinnest shell nanowire is observed. The results of these model calculations are consistent with our experimental observations of an enhanced FE piezoelectric response shown in Figure 1 and Figure 2a.

The observed shifts in the hysteresis loops (Figure 2c,d) results may be compared with those in which engineered strain, composition, or temperature gradients in planar single-layer and multilayer FE thin films result in polarization gradients, variations in polarization charge offset and T_C, and temperature dependence of the dielectric permittivity.[23] Electrostatic potential profiles $V(\rho)$ associated with polarization gradients resulting in a bound charge density were obtained using the calculated polarization profiles by numerically solving Poisson's equation assuming open-circuit boundary conditions. The measured vertical shift in the FE piezoelectric hysteresis loops and the results of model calculation of offsets in polarization exhibit an increase for progressively smaller diameters and thinner shells (Figure 2c). The variations in the values of the measured voltage and model-calculated potential offsets are in reasonable agreement (Figure 2d). A small, fixed portion of the observed offset can be attributed to the Au core and Pt probe tip metal work-function difference, offset by possible contributions from molecular adsorbates between the Pt tip and nanoshell,[8] from nanoshell curvature-dependent variation in the effective contact area of the proximal probe tip with the nanoshell surface,[27] and from asymmetric leakage currents.[28]

An additional finite-diameter-dependent source of offset in polarization (and voltage) owing to the finite-size scaling of radial stress and resulting orthogonal strain gradient may contribute to the observed polarization. In piezoelectric materials, in addition to the coupling of a mechanical stress, an additional but normally small contribution to dielectric or ferroelectric polarization results from a strain gradient,[29] i.e.

$$P_i = d_{ijk}\sigma_{jk} + \mu_{ijkl}(\partial\epsilon_{jk}/\partial x_l)$$

where μ_{ijkl} is the flexoelectric tensor. Considering the scale of values of μ_{ijkl} for PZT (≈0.5–2.0 μC /m)[29] an estimate of the magnitude of this effect based on our model calculations results in much larger offsets than those observed experimentally; we propose that defects partially relieve the high radial stress (and strain gradient), thereby providing offset values that are in better agreement with our experimental results.

Finally, a surface chemical mechanism[2,5,8] relevant to both the FE stability and offsets in the FE hysteresis response that are observed should be noted; molecular adsorbates can be expected to be present on the outer surface of the nanoshells. Adsorbates have been shown both to stabilize ferroelectricity and to introduce asymmetry to the polarization-energy landscape.[8] These effects are not included in the model calculations.

To conclude, we propose that our findings of significantly enhanced FE piezoelectric responses and the absence of a systematic decrease for decreasing shell thickness for polarizations oriented along the finite dimension in extremely curved ultrathin shells are explained by stress-renormalized and polarization gradient contributions to the free energy. These gradients, manifested in the form of geometrically driven preferred polarization direction and electrostatic potential offsets, produce significant finite curvature-dependent increases in T_C.

Acknowledgment. We thank Anna Morozovska, Andrew M. Rappe, Ilya Grinberg, Wissam Al-Saidi, and Shari L. Moskow for helpful discussions, and Terrence McGuckin for the design and construction of a sample interface. The authors gratefully acknowledge support for this work from the U.S. Army Research Office (W911NF-08-1-0067). S.S.N. and E.G. were supported in part by the NSF-IGERT (DGE-0221664) and NSF GK-12 (DGE-0538476) and by an NSF Graduate Research Fellowship (E.G.).

DOI: 10.1021/nl903384p | *Nano Lett.* **2010,** *10,* 542-546

Supporting Information Available. Additional information on device fabrication, the proximal probing experimental method, conditions, and analysis and details of the numberical calcualtions formed. This material is available free of charge via the Internet at http://pubs.acs.org.

REFERENCES AND NOTES

(1) Warusawithana, M. P.; Cen, C.; Sleasman, C. R.; Woicik, J. C.; Li, Y.; Kourkoutis, L. F.; Klug, J. A.; Li, H.; Ryan, P.; Wang, L.-P.; et al. *Science* **2009**, *324*, 367.

(2) Wang, R. V.; Fong, D. D.; Jiang, F.; Highland, M. J.; Fuoss, P. H.; Thompson, C.; Kolpak, A. M.; Eastman, J. A.; Streiffer, S. K.; Rappe, A. M.; et al. *Phys. Rev. Lett.* **2009**, *102*, 047601.

(3) Sai, N.; Fennie, C. J.; Demkov, A. A. *Phys. Rev. Lett.* **2009**, *102*, 107601.

(4) Choi, K. J.; Biegalski, M.; Li, Y. L.; Sharan, A.; Schubert, J.; Uecker, R.; Reiche, P.; Chen, Y. B.; Pan, X. Q.; Gopalan, V.; et al. *Science* **2004**, *306*, 1005.

(5) Fong, D. D.; Kolpak, A. M.; Eastman, J. A.; Streiffer, S. K.; Fuoss, P. H.; Stephenson, G. B.; Thompson, C.; Kim, D. M.; Choi, K. J.; Eom, C. B.; et al. *Phys. Rev. Lett.* **2006**, *96*, 127601.

(6) Garcia, V.; Fusil, S.; Bouzehouane, K.; Enouz-Vedrenne, S.; Mathur, N.; Barthelemy, A.; Bibes, M. *Nature* **2009**, *460*, 81.

(7) Maksymovych, P.; Jesse, S.; Yu, P.; Ramesh, R.; Baddorf, A. P.; Kalinin, S. *Science* **2009**, *324*, 1421.

(8) Spanier, J.; Kolpak, A.; Urban, J.; Grinberg, I.; Ouyang, L.; Yun, W.; Rappe, A.; Park, H. *Nano Lett.* **2006**, *6*, 735.

(9) Scott, J. F. *Science* **2007**, *315*, 954.

(10) Naumov, I. I.; Bellaiche, L.; Fu, H. *Nature* **2004**, *432*, 737.

(11) Morozovska, A. N.; Eliseev, E. A.; Glinchuk, M. D. *Physica B* **2007**, *387*, 358.

(12) Stengel, M.; Vanderbilt, D.; Spaldin, N. A. *Nat. Mater.* **2009**, *8*, 392.

(13) Rodriguez, B. J.; Gao, X. S.; Liu, L. F.; Lee, W.; Naumov, I. I.; Bratkovsky, A. M.; Hesse, D.; Alexe, M. *Nano Lett.* **2009**, *9*, 1127.

(14) Yadlovker, D.; Berger, S. *Phys. Rev. B* **2005**, *71*, 184112.

(15) Wang, Z.; Hu, J.; Yu, M.-F. *Appl. Phys. Lett.* **2006**, *89*, 263119.

(16) Urban, J. J.; Spanier, J. E.; Ouyang, L.; Yun, W. S.; Park, H. *Adv. Mater.* **2003**, *15*, 423.

(17) Nonnenmann, S. S.; Gallo, E. M.; Soja, G. R.; Coster, M. T.; Joseph, R. S.; Johnson, C. L.; Spanier, J. E. *Appl. Phys. Lett.* **2009**, *95*, 232903.

(18) Gruverman, A.; Tokumoto, H.; Prakash, A. S.; Aggarwal, S.; Yang, B.; Wuttig, M.; Ramesh, R.; Auciello, O.; Venkatesan, T. *Appl. Phys. Lett.* **1997**, *71*, 3492.

(19) Devonshire, A. *Adv. Phys.* **1954**, *3*, 85.

(20) Nagarajan, V.; Jia, C. L.; Kohlstedt, H.; Waser, R.; Misirlioglu, I. B.; Alpay, S. P.; Ramesh, R. *Appl. Phys. Lett.* **2005**, *86*, 192910.

(21) Pertsev, N. A.; Rodriguez-Contreras, J.; Kukhar, V. G.; Hermanns, B.; Kohlstedt, H.; Waser, R. *Appl. Phys. Lett.* **2003**, *83*, 3356.

(22) Tagantsev, A. K.; Stolichnov, I. A. *Appl. Phys. Lett.* **1999**, *74*, 1326.

(23) Ban, Z.-G.; Alpay, S. P.; Mantese, J. V. *Phys. Rev. B.* **2003**, *67*, 184104.

(24) Haun, M.; Furman, E.; Jang, S.; McKinstry, H.; Cross, L. *J. Appl. Phys.* **1987**, *62*, 3331.

(25) Kim, D.; Maria, J.; Kingon, A.; Streiffer, S. *J. Appl. Phys.* **2003**, *93*, 5568.

(26) Bratkovsky, A. P.; Levanyuk, A. M. *Phys. Rev. Lett.* **2005**, *94*, 107601.

(27) Hong, S.; Shin, H.; Woo, J.; No, K. *Appl. Phys. Lett.* **2002**, *80*, 1453.

(28) Bouregba, R.; Poullain, G.; Vilquin, B.; Rhun, G. L. *J. Appl. Phys.* **2003**, *93*, 5583.

(29) Ma, W.; Cross, L. E. *Appl. Phys. Lett.* **2003**, *82*, 3293.

DOI: 10.1021/nl903384p | *Nano Lett.* **2010,** *10,* 542-546